

# Microstructural Features and Functional Properties of Bilayered BaTiO<sub>3</sub>/BaTi<sub>1-x</sub>Zr<sub>x</sub>O<sub>3</sub> Ceramics

Thiago Martins Amaral,<sup>‡,†</sup> Eduardo Antonelli,<sup>¶</sup> Diego Alejandro Ochoa,<sup>§</sup> José Eduardo García,<sup>§</sup> and Antonio Carlos Hernandez<sup>‡</sup>

<sup>‡</sup>Grupo de Crescimento de Cristais e Materiais Cerâmicos, Physics Institute of São Carlos, University of São Paulo, São Carlos, São Paulo 13560-970 Brazil

<sup>§</sup>Department of Applied Physics, Universitat Politècnica de Catalunya, BarcelonaTech, Barcelona 08034, Spain

<sup>¶</sup>Science and Technology Institute, Federal University of São Paulo, UNIFESP, São José dos Campos, São Paulo, Brazil

**Validity of mixture rule for dielectrics in series configuration and the correlation between microstructure and electrical properties in bilayered BaTiO<sub>3</sub>/BaTi<sub>1-x</sub>Zr<sub>x</sub>O<sub>3</sub> ceramics were studied. Samples were obtained from BaTi<sub>1-x</sub>Zr<sub>x</sub>O<sub>3</sub> (BTZ<sub>x</sub>) nanopowder synthesized by the polymeric precursor technique and had their microstructure, dielectric, piezoelectric, and ferroelectric properties investigated. These bilayered ceramics' properties were compared to the properties of homogeneous BTZ<sub>x</sub> samples. And, also, the formers' electrical permittivities were compared with the predictions of the simple mixture rule. According to the results, the microstructures of the layers do not differ from the microstructure of the corresponding homogeneous BTZ<sub>x</sub> ceramic. And pyroelectric coefficient measurements show that the electrical properties of the interface do not contribute to the functional properties of the bilayered samples. Nevertheless, on increasing Zr<sup>4+</sup>, the agreement between the experimental and the predicted permittivity of the bilayered ceramics is gradually reduced, mainly at temperatures where the permittivity is governed by the response of the layer containing Zr<sup>4+</sup>. As a mechanical joint between the layers, the interface induces stresses during sintering due to thermal mismatch between compositions, thereby affecting the bilayers' electrical properties. Our results show that interface's mechanical effects compromise the functional properties of layered ferroelectric ceramics.**

## I. Introduction

Barium titanate (BaTiO<sub>3</sub>) is a perovskite type (ABO<sub>3</sub>) ferroelectric material that has been known since the 1940s.<sup>1</sup> However, it still attracts much attention as a promising and environmentally friendly material for a variety of electronic devices such as capacitors, memory storage systems, piezoelectric, pyroelectric, and microwave components.<sup>2,3</sup> In fact, BaTiO<sub>3</sub> is nowadays the base material for most capacitors,<sup>4,5</sup> particularly for multilayer ceramic capacitors. To meet the technological requirements that these capacitors must satisfy, that is, high electrical permittivity, low dielectric loss, and temperature stability of properties, BaTiO<sub>3</sub> must be modified.<sup>6</sup> Among the possible modifications, the substitution of Ti<sup>4+</sup> ion by the larger ionic radius Zr<sup>4+</sup> in the B site leads to the solid solution compound BaTi<sub>1-x</sub>Zr<sub>x</sub>O<sub>3</sub> (BTZ<sub>x</sub>).<sup>7</sup>

When compared with the BaTiO<sub>3</sub>, this solid solution has reduced dielectric losses due to the higher chemical stability of the Zr<sup>4+</sup> ion. And, furthermore, the Curie temperature of the BTZ system gradually decreases as the zirconium content increases, whereas (for Zr<sup>4+</sup> substitutions greater than 15%) the electrical permittivity peak broadens in temperature due to an increase in the diffusive character of the ferroelectric to paraelectric phase transition.<sup>8–10</sup>

A way to increase the range of temperature stability in capacitors was explored by Ota *et al.*, by means of the mixture rules, to design capacitors from laminar bulk ceramics with layers of Ba<sub>1-x</sub>Sr<sub>x</sub>TiO<sub>3</sub><sup>11</sup> and (1-x)PbMg<sub>1/3</sub>Nb<sub>2/3</sub>O<sub>3-x</sub>PbTiO<sub>3</sub>.<sup>12</sup> These mixture rules, reunited in 1986 by Newham,<sup>13</sup> predict the properties of a composite based on the properties and volumetric fractions of its linear, isotropic, and homogeneous components. Other works also turned their attention to studying laminar bulk ceramics of perovskite compounds. For instance, Gopalan *et al.* focused their research on ionic transport and vacancy generation through the interface between BaTiO<sub>3</sub>-SrTiO<sub>3</sub> diffusion couples<sup>14</sup> and between layers of BaTi<sub>0.7</sub>Zr<sub>0.3</sub>O<sub>3</sub> and BaTi<sub>0.3</sub>Zr<sub>0.7</sub>O<sub>3</sub>.<sup>15</sup> Furthermore, Siao *et al.*<sup>16</sup> studied interdiffusion and Kirkendall porosity in bilayered BaTiO<sub>3</sub>/SrTiO<sub>3</sub> ceramics, whereas Maurya *et al.*<sup>17</sup> studied the piezoelectric and ferroelectric properties of layered BaTiO<sub>3</sub>/0.975BaTiO<sub>3</sub>-0.025Ba(Cu<sub>1/3</sub>Nb<sub>2/3</sub>)O<sub>3</sub> ceramics. Nevertheless, none of these authors considered the correlations between microstructural features of these bulk-layered ceramics and their functional properties, for example, the correlation between the interface characteristics and the electrical properties.

The aim of this work was to investigate microstructural, dielectric, ferroelectric, and piezoelectric properties of bilayered bulk BaTiO<sub>3</sub>/BaTi<sub>1-x</sub>Zr<sub>x</sub>O<sub>3</sub> ceramics. Special interest is given to the correlation between their microstructure and functional properties. And validation of the mixture rule for this system is also investigated, with the aim of making a tool available for designing more complex BaTiO<sub>3</sub>-based layered ceramics for specific demands.

## II. Experimental Procedure

BaTi<sub>1-x</sub>Zr<sub>x</sub>O<sub>3</sub> ( $x = 0, 0.05, 0.1$  and  $0.15$ ) powders were produced using the polymeric precursor route with Barium acetate (99%; Alpha Aesar, Ward Hill, MA), Ti(IV)-isopropoxide (97%; Sigma Aldrich, Saint Louis, MO), Zr(IV)-propoxide solution (70% Sigma Aldrich), citric acid (99.5%; Synth, Diadema, São Paulo, Brazil) and ethylene glycol (99.5%; Synth).<sup>18</sup> BaTi<sub>1-x</sub>Zr<sub>x</sub>O<sub>3</sub> ( $x = 0, 0.05, 0.1$  and  $0.15$ ) dense ceramics and bilayered BaTiO<sub>3</sub>/BaTi<sub>0.95</sub>Zr<sub>0.05</sub>O<sub>3</sub>, BaTiO<sub>3</sub>/BaTi<sub>0.9</sub>Zr<sub>0.1</sub>O<sub>3</sub> and BaTiO<sub>3</sub>/BaTi<sub>0.85</sub>Zr<sub>0.15</sub>O<sub>3</sub> ceramics were prepared by uniaxially pressing the powders under 30 MPa,

H. M. Chan—contributing editor

Manuscript No. 34980. Received May 11, 2014; approved December 2, 2014.

<sup>†</sup>Author to whom correspondence should be addressed. e-mails: thimara1@ursa.ifsc.usp.br; thimara1@gmail.com

one layer above the other, should that be the case, and then isostatically pressing at 350 MPa to produce disk-shaped samples (6 mm diameter and 1 mm thick). Then, the pellets were sintered at 1300°C for 2 h.

The microstructure was analyzed by scanning electron microscopy (SEM; Inspect F-50, FEI, Hillsboro, OR). The atomic concentration profile was obtained from line scan energy dispersive X-ray spectroscopy (EDX). The results from EDX analysis were used to confirm stoichiometry and estimate the interface and layer thicknesses and the volumetric fraction of each composition on the bilayered ceramics.

Samples electrodes were sputtered with gold for dielectric, ferroelectric, and piezoelectric measurements. The dielectric permittivity was measured in nonpolarized samples from room temperature to 150°C with rate of 1°C/min (FRA SI 1260 with dielectric interface 1296A, Solartron Analytical; Ametek, New York, NY). For the other measurements, samples were poled in an oil bath by applying an electric field of 2.0 kV/mm for 30 min at 25°C. The longitudinal piezoelectric coefficient is measured using a piezo- $d_{33}$  meter (PM3500; KCF Technologies, State College, PA) at room temperature. The pyroelectric coefficient was evaluated from the thermally stimulated depolarization current, measured by a Sub-Femtoamperimeter (Model 6430; Keithley, Cleveland, OH) at a heating rate of 5°C/min.

The relative thermal expansion of the homogeneous samples was measured in a dilatometer (DIL 402 PC; NETZSCH, Selb, Germany) under a thermal treatment equal to the sintering treatment. Results obtained during cooling from 1200°C to room temperature, and the reported value of the BaTiO<sub>3</sub>'s Young Modulus (67 GPa<sup>19</sup>), were used to estimate stress of the bilayered samples due to thermal mismatch between the layers.

### III. Results and Discussion

#### (1) BaTi<sub>1-x</sub>Zr<sub>x</sub>O<sub>3</sub> Ceramics

Scanning electron microscopy micrographs of BaTi<sub>1-x</sub>Zr<sub>x</sub>O<sub>3</sub> ceramics are shown in Figs. 1(a)–(d). As Zr<sup>4+</sup> substitution for Ti<sup>4+</sup> increases, the average grain size decreases from 33 μm in BaTiO<sub>3</sub> to less than 2 μm in BaTi<sub>0.85</sub>Zr<sub>0.15</sub>O<sub>3</sub>, pre-

sumably due to the slowest diffusion rate of Zr<sup>4+</sup>, that inhibits grain growth.<sup>20</sup> BaTi<sub>0.95</sub>Zr<sub>0.05</sub>O<sub>3</sub> has bimodal grain size distribution with average diameters of 13 and 2 μm, and BaTi<sub>0.9</sub>Zr<sub>0.1</sub>O<sub>3</sub> has an average grain size of 12 μm. No secondary phase or segregation is detected in grain boundaries.

Figure 2(a) shows the dielectric permittivity data at 1 kHz of BaTi<sub>1-x</sub>Zr<sub>x</sub>O<sub>3</sub> ceramics for temperatures from 25°C to 150°C. In this range of temperature, it is possible to observe: the tetragonal-to-cubic phase transition of the BaTiO<sub>3</sub>; the orthorhombic-to-tetragonal and the tetragonal-to-cubic phase

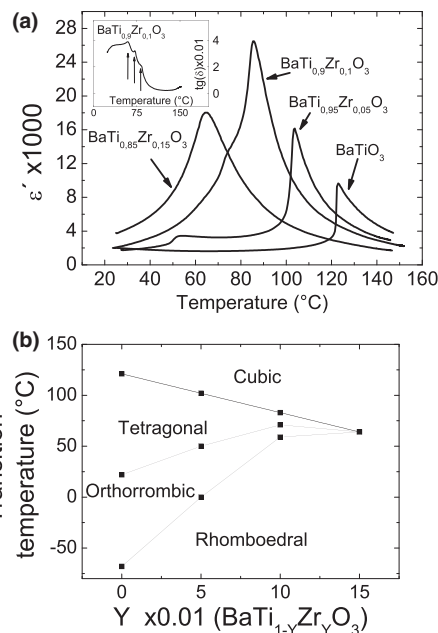


**Fig. 2.** (a) Temperature-dependent real permittivity of homogeneous BaTi<sub>1-x</sub>Zr<sub>x</sub>O<sub>3</sub> ( $x = 0, 0.05, 0.1,$  and  $0.15$ ) samples and; (b) phase transition temperatures evaluated by dielectric response. Temperature-dependent dielectric loss of BaTi<sub>0.9</sub>Zr<sub>0.1</sub>O<sub>3</sub> is shown in the inset of (a).

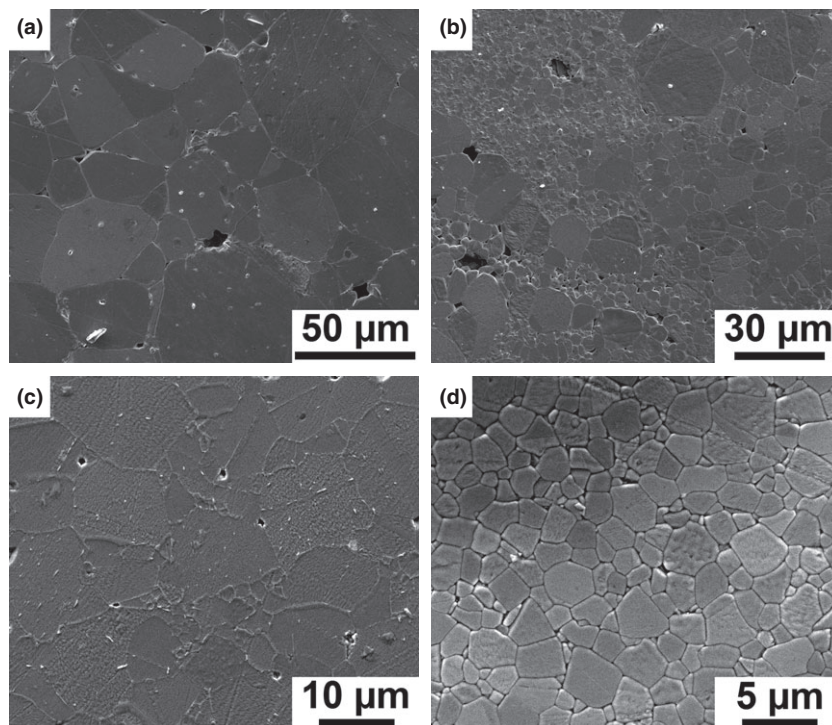


**Fig. 1.** SEM micrographs of homogeneous (a) BaTiO<sub>3</sub>, (b) BaTi<sub>0.95</sub>Zr<sub>0.05</sub>O<sub>3</sub>, (c) BaTi<sub>0.9</sub>Zr<sub>0.1</sub>O<sub>3</sub>, and (d) BaTi<sub>0.85</sub>Zr<sub>0.15</sub>O<sub>3</sub> ceramics.

transitions of the BaTi<sub>0.95</sub>Zr<sub>0.05</sub>O<sub>3</sub>; the rhombohedral-to-orthorhombic, the orthorhombic-to-tetragonal, and the tetragonal-to-cubic phase transitions of the BaTi<sub>0.9</sub>Zr<sub>0.1</sub>O<sub>3</sub> smeared out in the observable real permittivity peak; and the pinched rhombohedral-to-cubic phase transition of the BaTi<sub>0.85</sub>Zr<sub>0.15</sub>O<sub>3</sub>. The BaTi<sub>0.9</sub>Zr<sub>0.1</sub>O<sub>3</sub> phase transitions are better resolved in the dielectric loss temperature dependence of this composition, as shown in the inset. These data concerning the temperature dependence of the dielectric permittivities of homogeneous samples were used as input to the mixture rule to predict real dielectric permittivity values for the bilayered ceramics.

Figure 2(b) summarizes in a phase diagram the phase transition temperatures obtained for each BaTi<sub>1-x</sub>Zr<sub>x</sub>O<sub>3</sub> ceramic. On increasing Zr<sup>4+</sup> substitution of Ti<sup>4+</sup>, there is a gradual decrease in the Curie temperature and an increase in the temperatures of the other phase transitions. For 15% of Zr<sup>4+</sup> substitution, the three phase transitions merge together in a pinched phase transition, as also reported by other authors.<sup>10</sup> The difference between the ionic radius of Zr<sup>4+</sup> and Ti<sup>4+</sup>, when the former substitutes the latter, leads to a depressed displacement of Zr<sup>4+</sup> in B site of the O<sup>2-</sup> octahedra and to a weaker bonding with O<sup>2-</sup>. This results in a “break” of the cooperative vibrations of the B–O chains responsible for ferroelectricity in BaTiO<sub>3</sub>, which manifests itself macroscopically in the decrease in the Curie temperature and changes in the ferroelectric and piezoelectric properties of the BaTi<sub>1-x</sub>Zr<sub>x</sub>O<sub>3</sub> compounds.<sup>21,22</sup>

Table I summarizes the remanent polarization ( $P_r$ ), the coercive field ( $E_c$ ), and the piezoelectric coefficient ( $d_{33}$ ) for the BaTi<sub>1-x</sub>Zr<sub>x</sub>O<sub>3</sub> ceramics at 25°C. Values obtained by other authors<sup>2,8,21,23–25</sup> are included for comparison. The substitution of Ti<sup>4+</sup> for Zr<sup>4+</sup> hardens the ceramics and reduces their ferroelectric and piezoelectric properties. The BaTi<sub>0.95</sub>Zr<sub>0.05</sub>O<sub>3</sub> composition is an exception, because it presents its orthorhombic-to-tetragonal phase transition close to room temperature, maximizing their properties as a consequence of the polarization extension phenomenon.<sup>26</sup>

## (2) Bilayered BaTiO<sub>3</sub>/BaTi<sub>1-x</sub>Zr<sub>x</sub>O<sub>3</sub> Ceramics

Figure 3(a)–(c) shows SEM micrographs of bilayered BaTiO<sub>3</sub>/BaTi<sub>1-x</sub>Zr<sub>x</sub>O<sub>3</sub> ceramics together with their Zr concentration profile, their interface thickness and the volumetric fraction of each layer. Far from the interface, the layers have no microstructural and no chemical differences when compared with the corresponding homogeneous BaTi<sub>1-x</sub>Zr<sub>x</sub>O<sub>3</sub> ceramic, presenting the same average grain size (including bimodal grain size distribution in the BaTi<sub>0.95</sub>Zr<sub>0.05</sub>O<sub>3</sub> layer) and same composition. As the thicknesses of the layers are wider than the length of many grains, isotropic crystalline orientation of each layer is expected.<sup>13</sup> And no second phase segregation on grain boundary was detected. The interface, that is, the region between layers, is characterized by a change in Zr<sup>4+</sup> concentration with length and by a remanent porosity from material processing (also reported by other

**Table I. Remanent Polarization ( $P_r$ ), Coercive Field ( $E_c$ ), and Piezoelectric Coefficient ( $d_{33}$ ) Values Obtained for Homogeneous BaTi<sub>1-x</sub>Zr<sub>x</sub>O<sub>3</sub> Ceramics. Values from Other Authors are also Reported**

| Composition  | $P_r$ ( $\mu\text{C}/\text{cm}^2$ ) $\pm$ 0.3 |  | $E_c$ (kV/mm) $\pm$ 0.2 |  | $d_{33}$ (pC/N) $\pm$ 5 |                                    |
|--|---|--|-------------------------|--|-------------------------|------------------------------------|
| BaTiO <sub>3</sub>                                     | 9.8   | 5.45 <sup>23</sup>   | 3.8                     | 3.14 <sup>23</sup>   | 130                     | 190 <sup>2</sup>                   |
| BaTi <sub>0.95</sub> Zr <sub>0.05</sub> O <sub>3</sub> | 7.9   | 6.7, <sup>21</sup> 13.3, <sup>8</sup> 9.0, <sup>24</sup> 5.4 <sup>25</sup> | 3.6                     | 4.8, <sup>21</sup> 3.5, <sup>8</sup> 3.3, <sup>24</sup> 1.86 <sup>25</sup> | 162                     | 91, <sup>8</sup> 208 <sup>24</sup> |
| BaTi <sub>0.9</sub> Zr <sub>0.1</sub> O <sub>3</sub>   | 6.8   | 7, <sup>21</sup> 6.2, <sup>24</sup> 5.3 <sup>25</sup>                      | 2.6                     | 5.8, <sup>21</sup> 2.4, <sup>24</sup> 1.34 <sup>25</sup>                   | 120                     | 160 <sup>24</sup>                  |
| BaTi <sub>0.85</sub> Zr <sub>0.15</sub> O <sub>3</sub> | 4.5   | 5.4, <sup>21</sup> 2.0, <sup>8</sup> 3.1, <sup>24</sup> 3.6 <sup>25</sup>  | 1.5                     | 0.22, <sup>21</sup> 1.3, <sup>8</sup> 1.8, <sup>24</sup> 1.5 <sup>25</sup> | 70                      | 82, <sup>8</sup> 150 <sup>24</sup> |

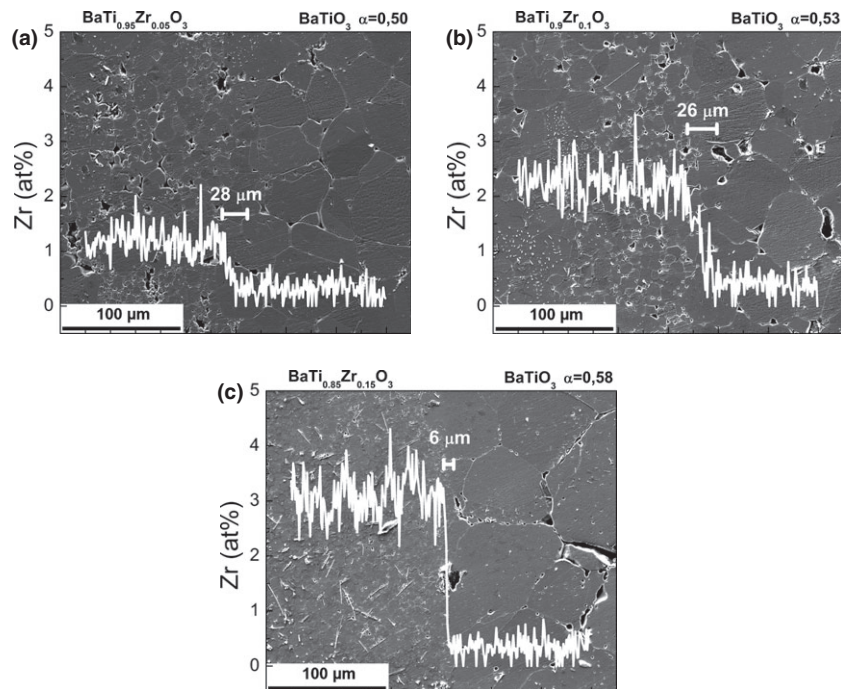


**Fig. 3.** SEM micrograph of bilayered (a) BaTiO<sub>3</sub>/BaTi<sub>0.95</sub>Zr<sub>0.05</sub>O<sub>3</sub>, (b) BaTiO<sub>3</sub>/BaTi<sub>0.9</sub>Zr<sub>0.1</sub>O<sub>3</sub>, and (c) BaTiO<sub>3</sub>/BaTi<sub>0.85</sub>Zr<sub>0.15</sub>O<sub>3</sub> ceramics. The composition, volumetric fraction ( $\alpha$ ), and interface thickness of each layer are displayed. Zirconium concentration profiles as a function of the longitudinal length are linked in the micrographs.



authors in bilayered BaTiO<sub>3</sub>/SrTiO<sub>3</sub> ceramics<sup>16</sup>). The interfaces of the BaTiO<sub>3</sub>/BaTi<sub>0.95</sub>Zr<sub>0.05</sub>O<sub>3</sub> and BaTiO<sub>3</sub>/BaTi<sub>0.9</sub>Zr<sub>0.1</sub>O<sub>3</sub> samples were observed to be thicker than that of the BaTiO<sub>3</sub>/BaTi<sub>0.85</sub>Zr<sub>0.15</sub>O<sub>3</sub>, probably because of the sizes of the grains in each adjacent layer that were available for coalescence processes during sintering. Table II summarizes the remanent polarization ( $P_r$ ), the coercive field ( $E_c$ ), and the piezoelectric coefficient ( $d_{33}$ ) for bilayered BaTiO<sub>3</sub>/BaTi<sub>1-x</sub>Zr<sub>x</sub>O<sub>3</sub> ceramics at 25°C. It is observed that the bilayered samples show intermediate ferroelectric and piezoelectric properties when compared with the corresponding homogeneous BaTi<sub>1-x</sub>Zr<sub>x</sub>O<sub>3</sub> ceramics. The fact that this layered design of ferroelectric ceramics does not improve properties related to remanent polarization was already reported<sup>17</sup> and it happens because of depolarizing fields at the interface between the layers.<sup>27</sup>

Figure 4 shows the temperature dependence of the pyroelectric coefficient for bilayered BaTiO<sub>3</sub>/BaTi<sub>1-x</sub>Zr<sub>x</sub>O<sub>3</sub> ceramics. For  $x = 0.05$  [Fig. 4(a)], the pyroelectric coefficient has three peaks around 50°C, 103°C, and 123°C, respectively, related to the transitions of the BaTi<sub>0.95</sub>Zr<sub>0.05</sub>O<sub>3</sub> and the transition of the BaTiO<sub>3</sub>. For  $x = 0.1$  [Fig. 4(b)], the pyroelectric coefficient has four peaks associated with the transitions of the BaTi<sub>0.9</sub>Zr<sub>0.1</sub>O<sub>3</sub> at 60°C, 70°C, and 82°C, and the transition of the BaTiO<sub>3</sub> at 123°C. The pyroelectric coefficient of BaTiO<sub>3</sub>/BaTi<sub>0.85</sub>Zr<sub>0.15</sub>O<sub>3</sub> [Fig. 4(c)] has two peaks, related to the pinched diffuse transition of the BaTi<sub>0.85</sub>Zr<sub>0.15</sub>O<sub>3</sub> around 65°C and to the ferroelectric-to-paraelectric phase transition of the BaTiO<sub>3</sub> at 123°C. The sharp observed peaks, associated with the layers of BaTiO<sub>3</sub>, BaTi<sub>0.95</sub>Zr<sub>0.05</sub>O<sub>3</sub>, and BaTi<sub>0.9</sub>Zr<sub>0.1</sub>O<sub>3</sub>, contrast with the broad peak associated with the BaTi<sub>0.85</sub>Zr<sub>0.15</sub>O<sub>3</sub> layer due to the diffuse character of the pinched phase transition of this last compound.<sup>9</sup> The temperature dependence of the pyroelectric coefficient presents no other signal besides those of the compositions of each layer, probably due to the small interface thickness when compared with the dimensions of the samples.

Figure 5 shows the temperature dependence of the real permittivity of the studied bilayered BaTiO<sub>3</sub>/BaTi<sub>1-x</sub>Zr<sub>x</sub>O<sub>3</sub> ceramics together with the predicted values obtained by the simple mixture rule. The volumetric fractions ( $\alpha$  and  $1-\alpha$ ) of each BaTi<sub>1-x</sub>Zr<sub>x</sub>O<sub>3</sub> layer and the temperature dependence of the permittivities ( $\epsilon_1$  and  $\epsilon_2$ ) of homogeneous samples fed the mixture rule, with the purpose of predicting the permittivity of the heterostructure ( $\epsilon$ ), according to the following equation for serial configuration:

$$\frac{1}{\epsilon} = \frac{\alpha}{\epsilon_1} + \frac{1-\alpha}{\epsilon_2}$$

As in the temperature dependence of the pyroelectric coefficient (Fig. 4), it is also possible to associate each permittivity peak of the bilayered ceramics displayed in Fig. 5 with the composition of each layer. Figure 5(a) shows the real permittivity of BaTiO<sub>3</sub>/BaTi<sub>0.95</sub>Zr<sub>0.05</sub>O<sub>3</sub>, where the peaks correspond to the two observable phase transitions of the BaTi<sub>0.95</sub>Zr<sub>0.05</sub>O<sub>3</sub> layer and to the one observable phase transition of the BaTiO<sub>3</sub> layer at 52°C, 102°C, and 122°C, respectively. Figure 5(b) shows the real permittivity of BaTiO<sub>3</sub>/BaTi<sub>0.9</sub>Zr<sub>0.1</sub>O<sub>3</sub>, where the three peaks correspond to the

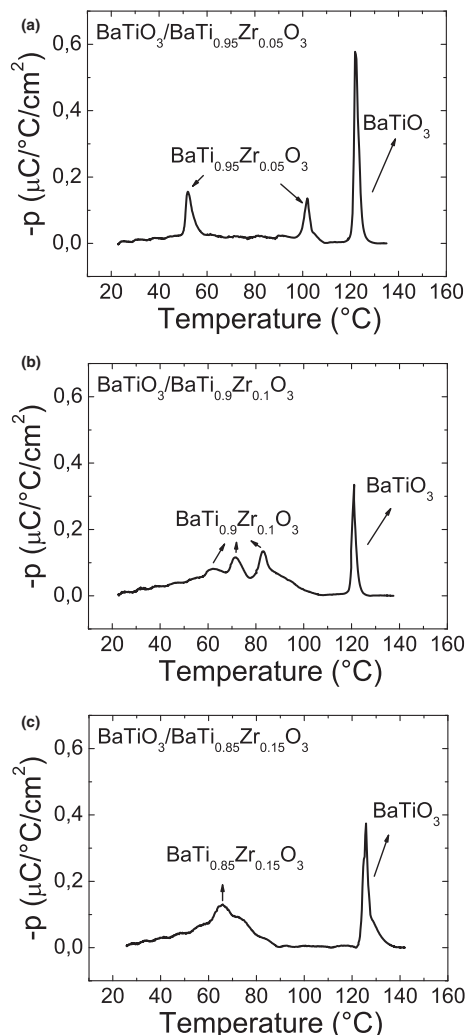


Fig. 4. Temperature-dependent pyroelectric coefficient of bilayered (a) BaTiO<sub>3</sub>/BaTi<sub>0.95</sub>Zr<sub>0.05</sub>O<sub>3</sub>, b) BaTiO<sub>3</sub>/BaTi<sub>0.9</sub>Zr<sub>0.1</sub>O<sub>3</sub>, and (c) BaTiO<sub>3</sub>/BaTi<sub>0.85</sub>Zr<sub>0.15</sub>O<sub>3</sub> ceramics identifying peaks corresponding to phase transitions of each layer composition.

phase transitions of the BaTi<sub>0.9</sub>Zr<sub>0.1</sub>O<sub>3</sub> layer and to that of the BaTiO<sub>3</sub> layer at 60°C, 70°C, 83°C, and 123°C, respectively. And the real permittivity of BaTiO<sub>3</sub>/BaTi<sub>0.85</sub>Zr<sub>0.15</sub>O<sub>3</sub> is displayed in Figure 5(c), where the peak corresponding to the diffuse phase transitions of the BaTi<sub>0.85</sub>Zr<sub>0.15</sub>O<sub>3</sub> layer can be identified as well as that of the BaTiO<sub>3</sub> layer at 66°C and 123°C, respectively.

It is observed that, in the temperature range where phase transitions of BaTi<sub>0.9</sub>Zr<sub>0.1</sub>O<sub>3</sub> take place (i.e., around 60°C and 90°C), the permittivity peaks [Fig. 5(b)] are smoothed out, whereas the pyroelectric peaks [Fig. 4(b)] are sharp peaks. When designing permittivity versus temperature profiles, a smoothed dielectric response is expected when ferroelectric/ferroelectric transitions are close one to the other with respect to temperature. However, a sharp pyroelectric peak appears in a phase transition when the polarization

Table II. Remanent Polarization ( $P_r$ ), Coercive Field ( $E_c$ ), Piezoelectric Coefficient ( $d_{33}$ ) Values, and Estimated Maximum Stress in BaTiO<sub>3</sub> Layer Due to Thermal Mismatch ( $\sigma$ ) for the Bilayered BaTiO<sub>3</sub>/BaTi<sub>1-x</sub>Zr<sub>x</sub>O<sub>3</sub> Ceramics

| Sample   | $P_r$ ( $\mu\text{C}/\text{cm}^2$ ) $\pm 0.3$ | $E_c$ (kV/mm) $\pm 0.2$ | $d_{33}$ (pC/N) $\pm 5$ | $\sigma$ (MPa) |
|--|---|-------------------------|-------------------------|----------------|
| BaTiO <sub>3</sub> /BaTi <sub>0.95</sub> Zr <sub>0.05</sub> O <sub>3</sub> | 8.9   | 3.4                     | 123                     | 8              |
| BaTiO <sub>3</sub> /BaTi <sub>0.9</sub> Zr <sub>0.1</sub> O <sub>3</sub>   | 9.5   | 2.6                     | 111                     | 102            |
| BaTiO <sub>3</sub> /BaTi <sub>0.85</sub> Zr <sub>0.15</sub> O <sub>3</sub> | 8.4   | 2.1                     | 98                      | 164            |

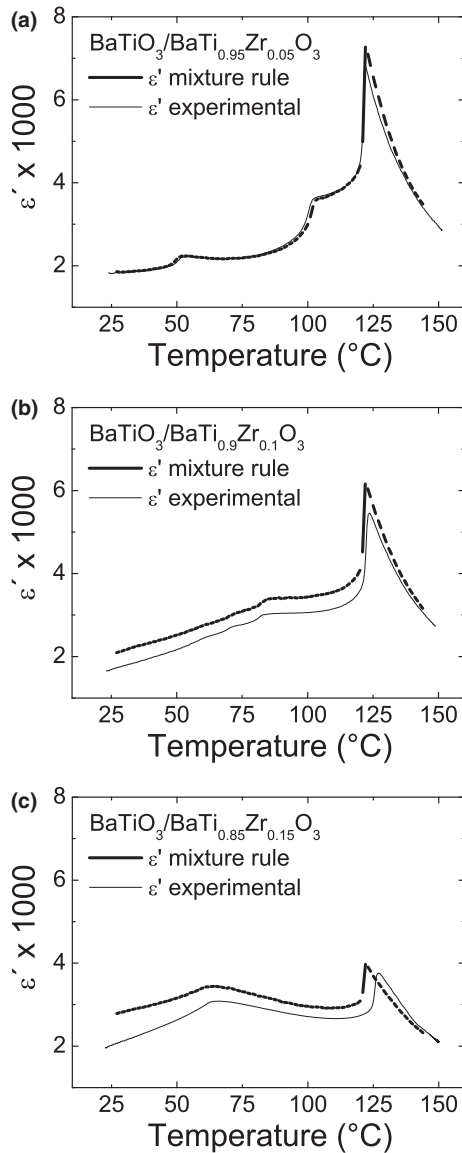


Fig. 5. Experimental and predicted temperature-dependent real permittivity of bilayered (a)  $\text{BaTiO}_3/\text{BaTi}_{0.95}\text{Zr}_{0.05}\text{O}_3$ , (b)  $\text{BaTiO}_3/\text{BaTi}_{0.9}\text{Zr}_{0.1}\text{O}_3$ , and (c)  $\text{BaTiO}_3/\text{BaTi}_{0.85}\text{Zr}_{0.15}\text{O}_3$  ceramics.

suddenly changes to adapt to the new unit cell of the material. And also it is expected that, in the temperature range between phase transitions, scarce pyroelectric response will occur due only to thermal depolarization.

The predictions for the electrical permittivity by the simple mixture rule sufficiently agree with the experimental results for the studied samples, which means that the unpoled bilayered ceramics may be regarded as isotropic, homogeneous, and linear media while 1 V/mm is applied, and that many layers of different  $\text{BaTi}_{1-x}\text{Zr}_x\text{O}_3$  compositions could be stacked together in specific volumetric fractions to design a desired electrical permittivity temperature profile, as done by Ota *et al.* with other compositions.<sup>11,12</sup> Nevertheless, two features should be pointed out while analyzing Fig. 5; first, there is an increase in the disagreement between experimental and predicted permittivities on increasing  $\text{Zr}^{4+}$  content in one of the layers, and second, the experimental values deviate more from the predicted in temperatures where the phase transitions of the  $\text{BaTi}_{1-x}\text{Zr}_x\text{O}_3$  ( $x \neq 0$ ) layer occur. These observations concerning mixture rule validity under low electrical field can be explained by assuming that the interface introduces stress while being a mechanical joint during cosintering of the layers. Other authors<sup>17</sup> also assumed that stresses were present in their bilayered and trilayered samples.

The estimated stresses in the  $\text{BaTiO}_3$  layer due to thermal mismatch on the studied samples are shown in the last column of Table II. As it is accepted that there is a stress gradient on the samples, these values would correspond to the maximum stress present.<sup>28</sup> It is observed that stress increases as  $\text{Zr}^{4+}$  substitution increases in the sample's  $\text{BaTi}_{1-x}\text{Zr}_x\text{O}_3$  ( $x \neq 0$ ) layer. According to the literature,<sup>29–33</sup> the phase transition temperatures and ferroelectric and piezoelectric properties of  $\text{BaTiO}_3$  are affected by applied stresses, and, furthermore, on a recent work<sup>34</sup> it was observed that  $\text{BaTi}_{1-x}\text{Zr}_x\text{O}_3$  has functional properties more susceptible to stress than  $\text{BaTiO}_3$ . So, in our bilayered  $\text{BaTiO}_3/\text{BaTi}_{0.95}\text{Zr}_{0.05}\text{O}_3$  ceramics, there is less  $\text{Zr}^{4+}$  and the smallest observed stress, thus, its electrical properties are less compromised by stresses and the predictions of the simple mixture rule agree well with the experimental results. Nevertheless, with further increase in  $\text{Zr}^{4+}$  content, the stress on the samples increases and the samples become more susceptible to the stresses effects. Thus, their functional properties are compromised and the agreement between experimental results and predictions of the simple mixture rule is gradually lost, mainly where the contribution from  $\text{BaTi}_{1-x}\text{Zr}_x\text{O}_3$  ( $x \neq 0$ ) layer on the electrical permittivity is greater than the  $\text{BaTiO}_3$ 's contribution, as observed, for example, close to the phase transition temperatures of  $\text{BaTi}_{1-x}\text{Zr}_x\text{O}_3$  ( $x \neq 0$ ).

#### IV. Conclusions

Microstructure, piezoelectric, ferroelectric, and dielectric properties of the bilayered  $\text{BaTiO}_3/\text{BaTi}_{1-x}\text{Zr}_x\text{O}_3$  ceramics are reported, correlated, and compared with properties of homogeneous  $\text{BaTi}_{1-x}\text{Zr}_x\text{O}_3$  samples. The interface joined the layers together, constraining the sintering process and inducing stress due to thermal mismatch between compositions. When there is small thermal mismatch stresses, it was shown that these layered ceramics could be used to smooth permittivity temperature behavior and that the mixture rule predictions holds for bilayered  $\text{BaTiO}_3/\text{BaTi}_{1-x}\text{Zr}_x\text{O}_3$  ceramics. Nevertheless, as the  $\text{Ti}^{4+}$  substitution increases, mixture rule predictions gradually lacked experimental correspondence due to increase in thermal mismatch stress and increase in the stresses effects over the properties of the  $\text{BaTi}_{1-x}\text{Zr}_x\text{O}_3$  layers.

#### Acknowledgments

The authors gratefully acknowledge financial support from FAPESP and CNPq, two Brazilian research-funding agencies. Support from the project MAT2013-48009-C4-2-P of the Spanish Government is also appreciatively acknowledged.

#### References

- G. H. Haertling, "Ferroelectric Ceramics: History and Technology," *J. Am. Ceram. Soc.*, **82** [4] 797–818 (1999).
- T. R. Shrout and S. J. Zhang, "Lead-Free Piezoelectric Ceramics: Alternatives for PZT?" *J. Electroceram.*, **19** [1] 111–24 (2007).
- T. Karaki, K. Yan, T. Miyamoto, and M. Adachi, "Lead-Free Piezoelectric Ceramics with Large Dielectric and Piezoelectric Constants Manufactured from  $\text{BaTiO}_3$  Nano-Powder," *Jpn. J. Appl. Phys.*, **46** [4] L97–8 (2007).
- H. Kishi, Y. Mizuno, and H. Chazono, "Base-Metal Electrode-Multilayer Ceramic Capacitors: Past, Present and Future Perspectives," *Jpn. J. Appl. Phys.*, Part 1, **42** [1] 1–15 (2003).
- A. C. Randall, "Scientific and Engineering Issues of the State-of-the-Art and Future Multilayer Capacitors," *J. Ceram. Soc. Jpn.*, **109** [1] 2–6 (2001).
- H.-W. Lee, M. S. H. Chu, and H.-Y. Lu, "Phase Mixture and Reliability of  $\text{BaTiO}_3$ -Based X7R Multilayer Ceramic Capacitors: X-Ray Diffractometry and Raman Spectroscopy," *J. Am. Ceram. Soc.*, **94** [5] 1556–62 (2011).
- D. Hennings, A. Schnell, and G. Simon, "Diffuse Ferroelectric Phase Transitions in  $\text{Ba}(\text{Ti}_{1-y}\text{Zr}_y)\text{O}_3$  Ceramics," *J. Am. Ceram. Soc.*, **65** [11] 539–44 (1982).
- Z. Yu, C. Ang, R. Guo, and A. S. Bhalla, "Piezoelectric and Strain Properties of  $\text{Ba}(\text{Ti}_{1-x}\text{Zr}_x)\text{O}_3$  Ceramics," *J. Appl. Phys.*, **92** [3] 1489–93 (2002).
- T. Maiti, R. Guo, and A. S. Bhalla, "Evaluation of Experimental Resume of  $\text{BaZrTi}_{1-x}\text{O}_3$  with Perspective to Ferroelectric Relaxor Family: An Overview," *Ferroelectrics*, **425** [1] 4–26 (2011).

- <sup>10</sup>T. Maiti, R. Guo, and A. S. Bhalla, "Structure-Property Phase Diagram of  $\text{BaZr}_x\text{Ti}_{1-x}\text{O}_3$  System," *J. Am. Ceram. Soc.*, **91** [6] 1769–80 (2008).
- <sup>11</sup>T. Ota, Y. Abe, T. Hirashita, H. Myazaki, Y. Hikichi, and H. Suzuki, "Flat Profile of Permittivity vs Temperature for Graded  $\text{Ba}_{1-x}\text{Sr}_x\text{TiO}_3$  Ceramics," *J. Ceram. Soc. Jpn.*, **109** [2] 174–6 (2001).
- <sup>12</sup>T. Ota, J. Fujita, S. Kimura, M. Mizutani, Y. Hikichi, H. Myazaki, and H. Suzuki, "Designing of Permittivity vs Temperature Profile for Functionally Graded  $f\text{X}$  PMN-PT," *J. Ceram. Soc. Jpn.*, **110** [9] 826–9 (2002).
- <sup>13</sup>R. E. Newnham, "Composite Electroceramics," *Ferroelectrics*, **68** [1] 1–32 (1986).
- <sup>14</sup>S. Gopalan and A. V. Virkar, "Interdiffusion and Kirkendall Effect in Doped Barium Titanate-Strontium Titanate Diffusion Couples," *J. Am. Ceram. Soc.*, **78** [4] 993–8 (1995).
- <sup>15</sup>S. Gopalan and A. V. Virkar, "Interdiffusion and Kirkendall Effect in Doped  $\text{BaTiO}_3$ - $\text{BaZrO}_3$  Perovskites: Effect of Vacancy Supersaturation," *J. Am. Ceram. Soc.*, **82** [10] 2887–99 (1999).
- <sup>16</sup>C.-Y. Siao, H.-W. Lee, and H.-Y. Lu, "Kirkendall Porosity in Barium Titanate-Strontium Titanate Diffusion Couple," *Ceram. Int.*, **35** [7] 2951–8 (2009).
- <sup>17</sup>D. Maurya, N. Wongdamern, R. Yimnirun, and S. Priya, "Dielectric and Ferroelectric Response of Compositionally Graded Bilayer and Trilayer Composites of  $\text{BaTiO}_3$  and  $0.975\text{BaTiO}_3$ - $0.025\text{Ba}(\text{Cu}_{1/3}\text{Nb}_{2/3})\text{O}_3$ ," *J. Appl. Phys.*, **108** [12] 124111, 10pp (2010).
- <sup>18</sup>M. I. B. Bernardi, E. Antonelli, A. B. Louren, C. A. C. Feitosa, L. J. Q. Maia, and A. C. Hernandez, " $\text{BaTi}_{1-x}\text{Zr}_x\text{O}_3$  Nanopowders Prepared by the Modified Pechini Method," *J. Therm. Anal. Calorim.*, **87** [3] 725–30 (2007).
- <sup>19</sup>T. Sakakibara, H. Izu, T. Kura, W. Shinohara, H. Iwata, S. Kiyama, and S. Tsuda, "High-Voltage Photovoltaic Micro-Devices Fabricated by a New Laser-Processing," *Proc. IEEE 5th Int. Symp. Micro Mach. Hum. Sci.*, **75**, 282–7 (1994).
- <sup>20</sup>S. Sarangi, T. Badapanda, B. Behera, and S. Anwar, "Frequency and Temperature Dependence Dielectric Behavior of Barium Zirconate Titanate Nanocrystalline Powder Obtained by Mechanochemical Synthesis," *J. Mater. Sci. Mater. Electron.*, **24** [10] 4033–42 (2013).
- <sup>21</sup>N. Sawangwan, J. Barrel, K. MacKenzie, and T. Tunkasiri, "The Effect of Zr Content on Electrical Properties of  $\text{Ba}(\text{Ti}_{1-x}\text{Zr}_x)\text{O}_3$  Ceramics," *Appl. Phys. A*, **90** [4] 723–7 (2007).
- <sup>22</sup>S. J. Kuang, X. G. Tang, L. Y. Li, Y. P. Jiang, and Q. X. Liu, "Influence of Zr Dopant on the Dielectric Properties and Curie Temperatures of  $\text{Ba}(\text{Zr}_x\text{Ti}_{1-x})\text{O}_3$  ( $0 \leq x \leq 0.12$ ) Ceramics," *Scr. Mater.*, **61** [1] 68–71 (2009).
- <sup>23</sup>S. Mahajan, O. P. Thakur, C. Prakash, and K. Sreenivas, "Effect of Zr on Dielectric, Ferroelectric and Impedance Properties of  $\text{BaTiO}_3$  Ceramic," *Bull. Mater. Sci.*, **34** [7] 1483–9 (2011).
- <sup>24</sup>W. Li, Z. Xu, R. Chu, P. Fu, and G. Zang, "Dielectric and Piezoelectric Properties of  $\text{Ba}(\text{Zr}_x\text{Ti}_{1-x})\text{O}_3$  Lead-Free Ceramics," *Brazilian J. Phys.*, **40** [3] 353–6 (2010).
- <sup>25</sup>F. Moura, a. Z. Simões, B. D. Stojanovic, M. a. Zaghete, E. Longo, and J. a. Varela, "Dielectric and Ferroelectric Characteristics of Barium Zirconate Titanate Ceramics Prepared from Mixed Oxide Method," *J. Alloys Compd.*, **462** [1–2] 129–34 (2008).
- <sup>26</sup>L. Dong, D. S. Stone, and R. S. Lakes, "Enhanced Dielectric and Piezoelectric Properties of  $\text{XBaZrO}_3$ - $(1-x)\text{BaTiO}_3$  Ceramics," *J. Appl. Phys.*, **111** [8] 084107, 10pp (2012).
- <sup>27</sup>J. V. Mantese and S. P. Alpay, *Graded Ferroelectrics, Transpacitors and Transponders*. Springer, New York, 2005.
- <sup>28</sup>R. Bermejo, C. Baudin, R. Moreno, L. Llanes, and A. Sanchezherencia, "Processing Optimisation and Fracture Behaviour of Layered Ceramic Composites with Highly Compressive Layers," *Compos. Sci. Technol.*, **67** [9] 1930–8 (2007).
- <sup>29</sup>S. Lin, T. Lü, C. Jin, and X. Wang, "Size Effect on the Dielectric Properties of  $\text{BaTiO}_3$  Nanoceramics in a Modified Ginsburg-Landau-Devonshire Thermodynamic Theory," *Phys. Rev. B*, **74** [13] 134115, 5pp (2006).
- <sup>30</sup>J. L. Zhu, S. Lin, S. M. Feng, L. J. Wang, Q. Q. Liu, C. Q. Jin, X. H. Wang, C. F. Zhong, L. T. Li, and W. Cao, "Pressure Tuned Ferroelectric Reentrance in Nano- $\text{BaTiO}_3$  Ceramics," *J. Appl. Phys.*, **112** [12] 124107, 4pp (2012).
- <sup>31</sup>W. Chaisan, R. Yimnirun, and S. Ananta, "Changes in Ferroelectric Properties of Barium Titanate Ceramic with Compressive Stress," *Phys. Scr.*, **129**, 205–8 (2007).
- <sup>32</sup>M. Demartin and D. Damjanovic, "Dependence of the Direct Piezoelectric Effect in Coarse and Fine Grain Barium Titanate Ceramics on Dynamic and Static Pressure," *Appl. Phys. Lett.*, **68** [21] 3046–8 (1996).
- <sup>33</sup>T. Sakashita, M. Deluca, S. Yamamoto, H. Chazono, and G. Pezzotti, "Stress Dependence of the Raman Spectrum of Polycrystalline Barium Titanate in Presence of Localized Domain Texture," *J. Appl. Phys.*, **101** [12] 123517, 12pp (2007).
- <sup>34</sup>T. Hoshina, T. Furuta, T. Yamazaki, H. Takeda, and T. Tsurumi, "Grain Size Effect on Dielectric Properties of  $\text{Ba}(\text{Zr}, \text{Ti})\text{O}_3$  Ceramics," *Jpn. J. Appl. Phys.*, **51**, 09LC04–1 (2012). □